Neuron, Volume *73*

Supplemental Information

Sound-Driven Synaptic Inhibition

in Primary Visual Cortex

Giuliano Iurilli, Diego Ghezzi, Umberto Olcese, Glenda Lassi, Cristiano Nazzaro, Raffaella Tonini, Valter Tucci, Fabio Benfenati, and Paolo Medini

Inventory of Supplemental items:

A. SUPPLEMENTAL FIGURES

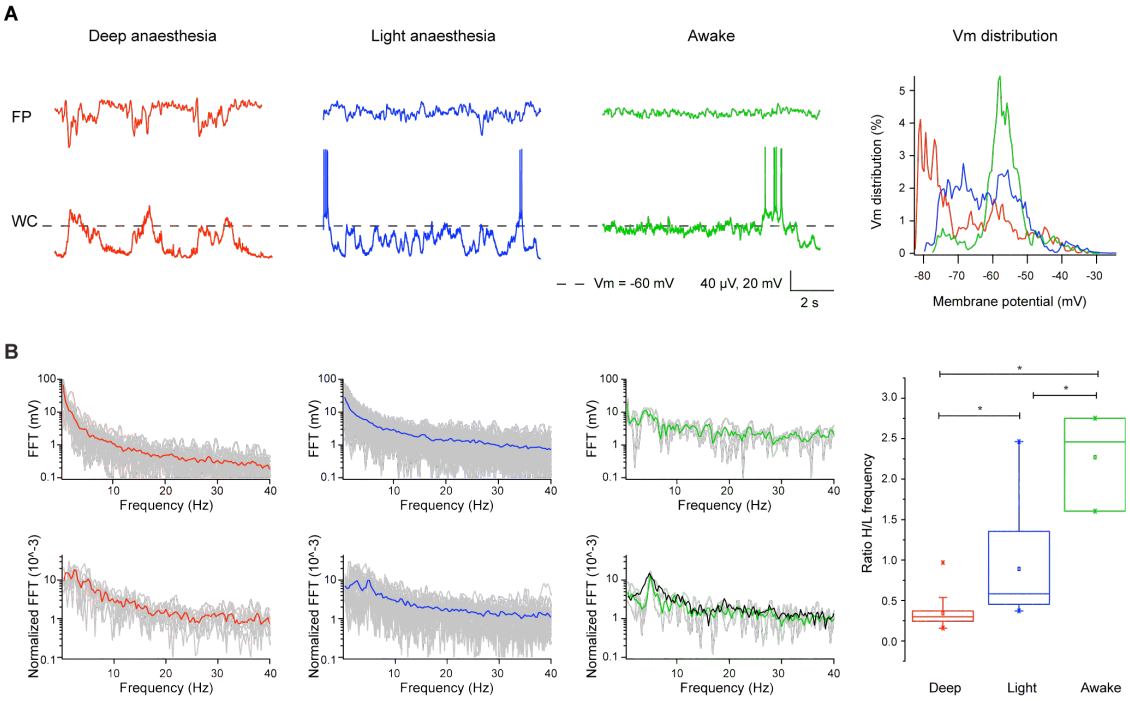

Figure S1. Electrophysiological monitoring of anaesthesia level. Related to Figure 1. (A) Simultaneous supragranular field potentials (FPs, upper traces) and whole-cell (WC) recordings of L2/3Ps (lower traces) from deeply anaesthetized (red, 1.8 g/Kg i.p. urethane), lightly anaesthetized (blue, 0.8-1 g/Kg i.p. urethane) and awake, head-fixed (green) mice. The right plot shows the percentage of time spent by cells at different V_m values over a period (10 s) of spontaneous activity. Deeply anaesthetized mice present a biphasic V_m distribution reflecting the presence of pronounced Up and Down States. V_m values were more depolarized and unimodally distributed in lightly anesthetized and awake mice. Intra-cortical FPs were more desynchronized in lightly anesthetized and awake mice compared to the deeply anaesthetized. (B) Top row: individual V_m FFT spectra of L2/3Ps in deeply anaesthetized (averaged in red, n = 25), lightly anaesthetized (blue, n = 103) and awake, head-fixed (green, n = 3) mice. Low

frequencies are relatively more prominent under deep anaesthesia, whereas high frequencies are relatively more prominent in awake mice. This difference was quantified by the ratio between the 10-40 Hz range and the 1-5 Hz range (H/L frequency ratio), becoming progressively larger from deep anaesthesia to wakefulness (rightmost plot; one-way ANOVA, * $p < 0.05$ for all comparisons). Bottom row: Individual FFT spectra (normalized by their respective integral) of supra-granular FP recordings in deeply anaesthetized (averaged in red, N = 9), lightly anesthetized (blue, N = 63) and awake, head-fixed (green, N = 3) mice. The black line is the average FFT spectrum for freely-moving mice (N = 6). Under deep anaesthesia the dominant frequency range is 1-3 Hz; under light urethane anaesthesia the dominant frequency range is between 4 and 6 Hz with a second peak between 2 and 3 Hz; in awake mice the dominant frequency range is 4-7 Hz. Note the similarity between the average FFT spectra of awake and freely moving mice.

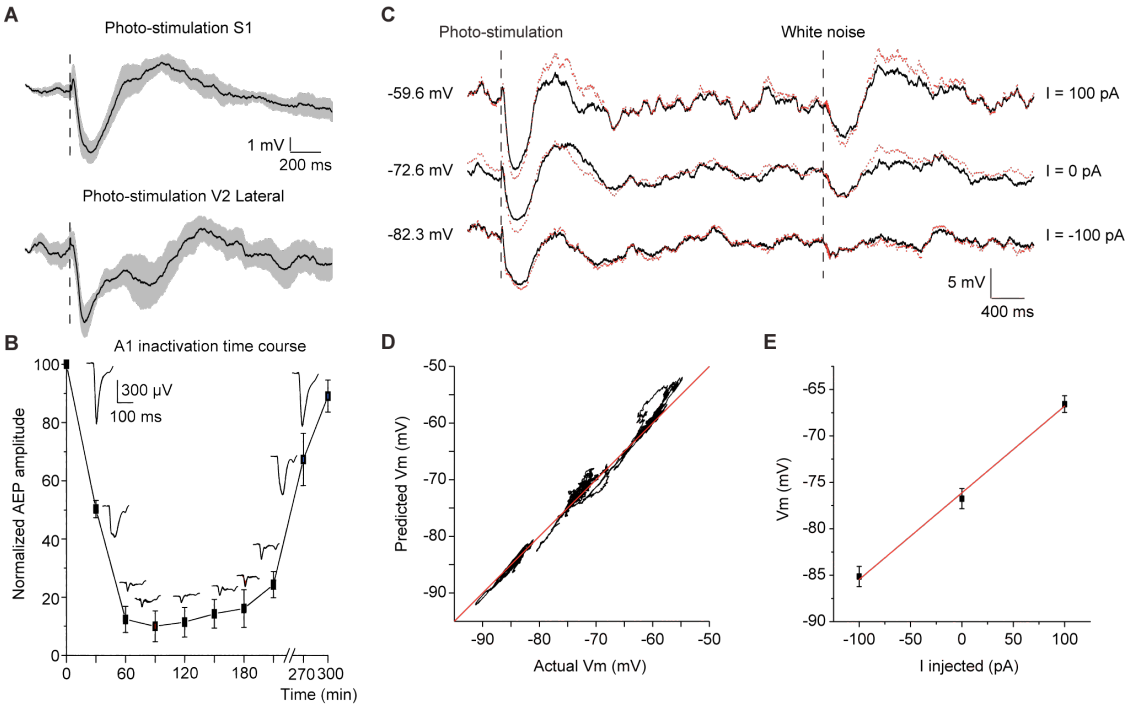

Figure S2. Widespread effects of inter-area photostimulation and estimates of excitatory and inhibitory conductances. Related to Figures 2 and 3. *(A) Nonspecific effects of cortical photostimulation.* Grand averages (mean V_m ± s.e.m.) of the intracellular responses of L2/3Ps of V1 to photostimulation of the barrel cortex (S1, top, n = 8) and of a visual association area located between A1 and V1 (V2 lateral, bottom; n = 6). In both cases robust hyperpolarizing responses were consistently evoked. (B) Time course of functional inactivation of A1 upon local muscimol injection measured by acoustically-evoked FPs (AEP). A1 inactivation was attained after 1 hr, and recovery of responsiveness occurred after ~ 5 hours. (C) Sub-threshold responses to photo-stimulation of A1 and to a noise burst under 3 different levels of current injection in a L2/3P of V1. The red dotted traces are the predicted V_m responses based on the estimated G_e and G_i. (D) Predicted V_m values plotted against the actual V_m values. In this example, the predicted values accounted for the 98 % of

the variance of the actual values. (E) The mean peak V_m values of the SH for the same cell were linearly related to current (I) injection values.

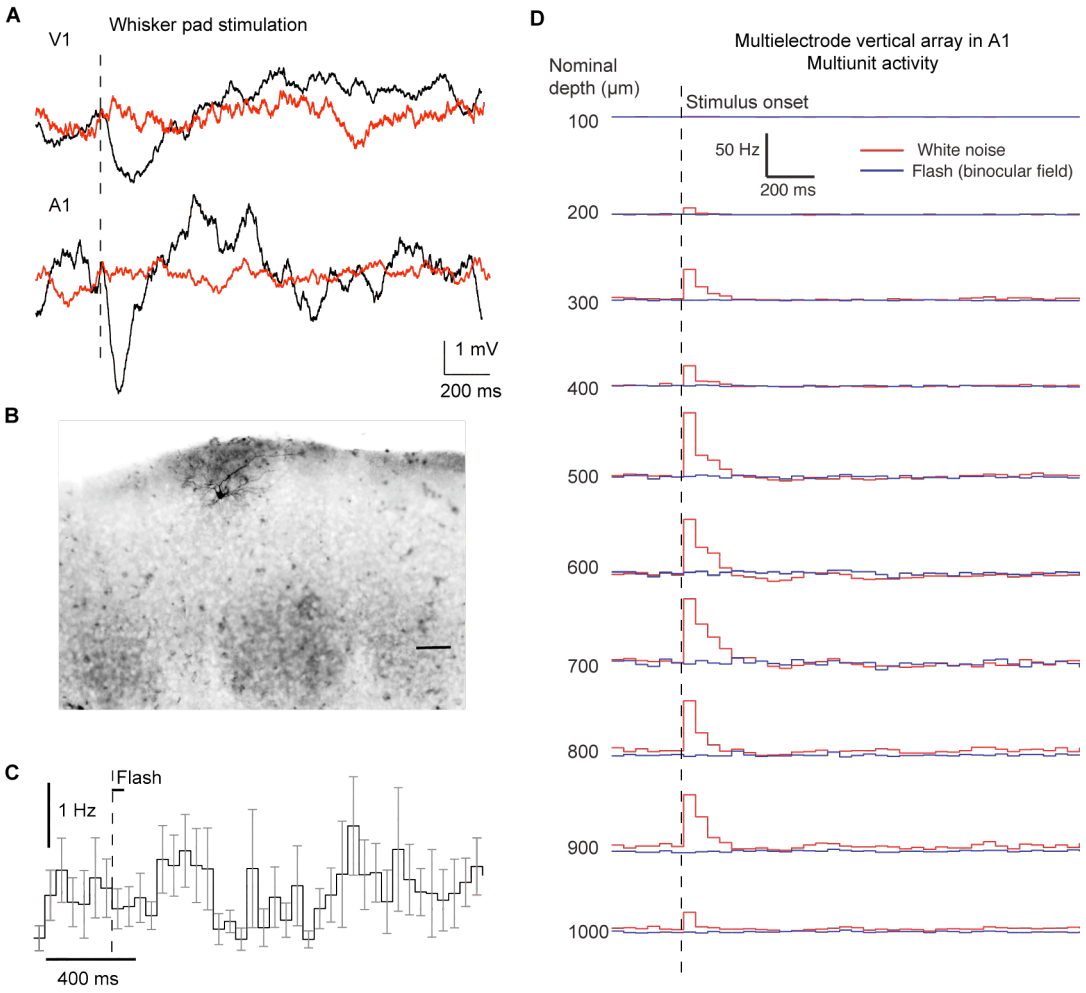

Figure S3. Controls for the specificity of piezo-driven hyperpolarizing responses and supra-threshold effects of visual stimuli in barrel and auditory cortex. Related to Figure 3. *(A) Piezo device activation per se did not cause subthreshold responses in L2/3Ps of V1 and A1.* Top: representative hyperpolarizing response evoked in a V1 L2/3P by multiwhisker stimulation (black). No response was evoked when the piezoelectric device was moved 1-2 mm off from the whisker tips (red). Bottom: representative hyperpolarizing response evoked in an A1 L2/3P by multiwhisker stimulation (black). Again, the mechanical stimulus generated by the movement of piezoelectric device did not evoke responses in absence of contact with

whiskers (red). In both cases the eyelids of the mouse were suture-closed and covered, whereas the ear canals were plugged with surgical cement. (B-D) *Effects of light stimuli in barrel and auditory cortex.* (B) Example of a biocytin-filled L2/3P in a barrel-related column (revealed with cytochrome C staining) responding with a small depolarization to a flash in the central binocular visual field. (C) Averaged PSTH (± s.e.m.) of action potential responses of L2/3Ps in S1 to visual stimulation (n = 13; dashed line: flash onset). Note the lack of detectable suprathreshold responses. Baseline (prestimulus) mean spike rate was 0.37 Hz. (D) Multi-unit activity along different recording sites (spaced every 100 μm) inserted along the depth of A1 in response to flashes or pattern reversals (blue) or to noise bursts (red, 3 mice). Note the lack of detectable AP responses in any site to visual stimuli, which contrasts with the robust auditory-driven responses.

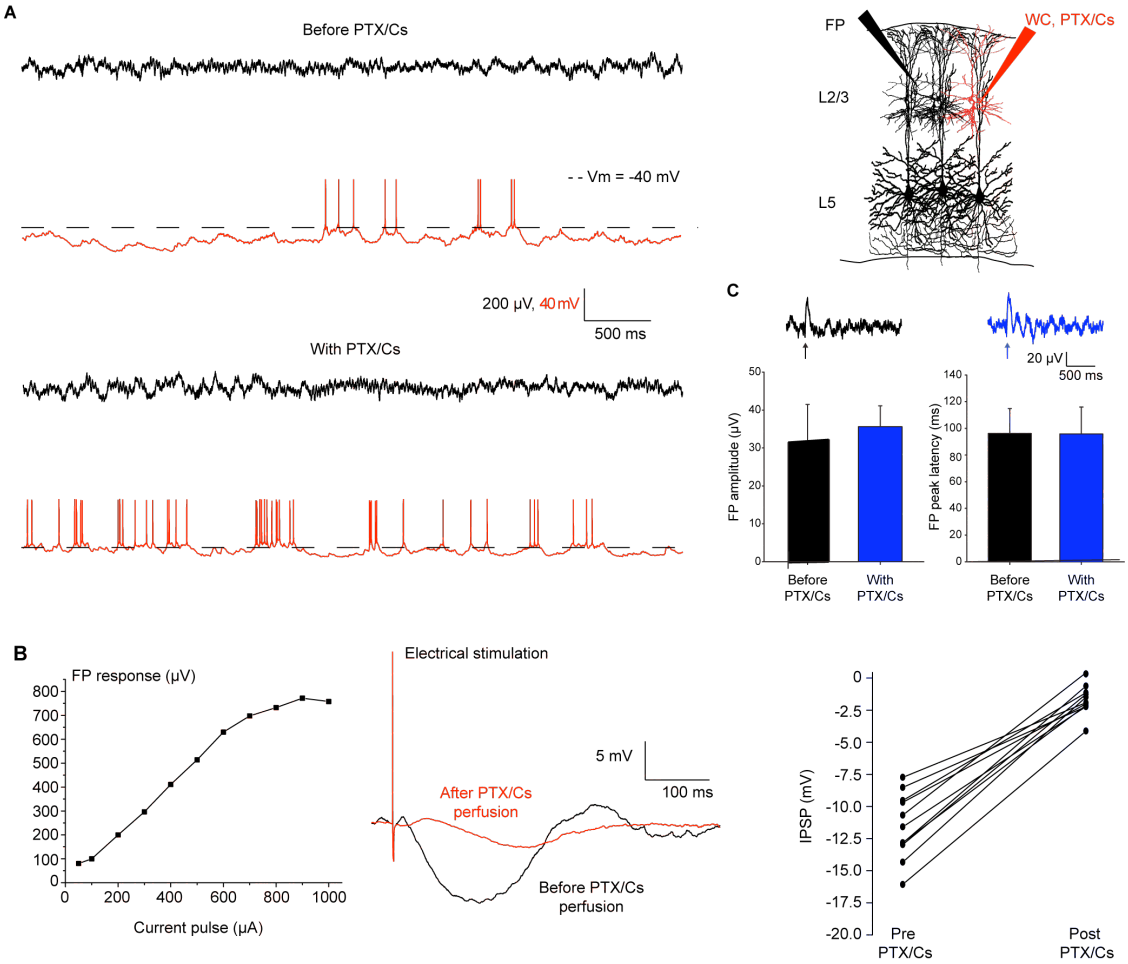
A
Before PTX/Cs
- - Vm = -40 mV
200 µV, 40 mV
500 ms
With PTX/Cs
FP
WC, PTX/Cs
L2/3
L5
C
20 µV
500 ms
FP amplitude (µV)
FP peak latency (ms)
Before PTX/Cs
With PTX/Cs
B
FP response (µV)
Current pulse (µA)
Electrical stimulation
5 mV
100 ms
After PTX/Cs perfusion
Before PTX/Cs perfusion
IPSP (mV)
Pre PTX/Cs
Post PTX/Cs
D
Control
Gabazine 1.5 µM
Gabazine 3 µM
CGP 1 µM
CGP 1 µM + Gabazine 1.5 µM
10 mV
500 ms
Vm = -50 mV
Vm distribution (%)
Membrane potential (mV)
E
Spontaneous firing (Hz)
Control
Gabazine 1.5 µM
Gabazine 3 µM
CGP 1 µM
CGP +Gabazine
F
Skweness
Control
Gabazine 1.5 µM
Gabazine 3 µM
CGP 1 µM
CGP +Gabazine

Figure S4. Controls for GABA blockade experiments. Related to Figure 4. (A) *Patching with PTX/Cs containing pipettes did not alter the intra-cortical FP.* Simultaneous in vivo whole-cell (WC) recordings with pipettes backfilled with PTX/Cs (red) and FP recordings (black). Patching with the GABA-blocking intracellular solution did not cause epileptiform activity. (B) *Intracellular perfusion with PTX/Cs abolished IPSPs caused by local cortical microstimulation*. Left: stimulus intensity for electrical stimulation was chosen to evoke a half-maximal local FP response. Middle: averaged intracellular responses to electrical stimulation immediately after patching (before PTX/Cs perfusion, black) and after 15 minutes from establishing the whole-cell configuration, to allow sufficient time for cell perfusion (after PTX/Cs perfusion, red). Resting V_m values were -67 and -22 mV before and after PTX/Cs perfusion, respectively. Right: PTX/Cs intracellular perfusion significantly counteracted microstimulation-driven IPSPs (paired t-test, $p < 0.001$). (C) *Patching with PTX/Cs containing pipettes did not affect the population synaptic response to sound in supragranular layers of V1.* The population synaptic response to sound (arrows are onsets) remained similar in terms of both amplitude (32.2 ± 9.3 vs 35.6 ± 5.5 μV) and latency (96.2 ± 18.7 vs 95.8 ± 20.2 ms) before and after patching with PTX/Cs (N = 8, paired *t*-tests, $p > 0.6$ for both). *(D-F) Effects of $GABA_A$ and $GABA_B$ receptor antagonists on spontaneous activity of L2/3Ps.* (D) Upper traces: representative examples of sweeps recorded from L2/3Ps of V1 during different regimes of GABA blockade. Note that gabazine increased firing rates at low concentration (1.5 μM), but only at higher concentration (3 μM) it caused epileptiform activity, characterized by short bursts of activity and long Down states. CGP52432 1 μM (CGP) also caused a smaller but significant increase of spontaneous firing rates. Significance level is 0.05. Bottom plots: corresponding distributions of V_m values over

time during spontaneous activity. The short Up states under high gabazine concentration skew the distribution towards more hyperpolarized membrane potential values. Dashed lines indicate the onset of the noise burst. Action potentials are truncated at -15 mV. (E) Spontaneous firing rates in controls and during CGP52432, low gabazine, gabazine-CGP52432 cocktail and high gabazine. Gabazine application significantly increased firing rates compared to both controls and CGP ($p < 0.05$) (F) Only high concentration of gabazine shortened Up states duration and elongated Down states as indicated by the larger skewness of the V_m distributions in time compared to all remaining groups ($p = 0.001$).

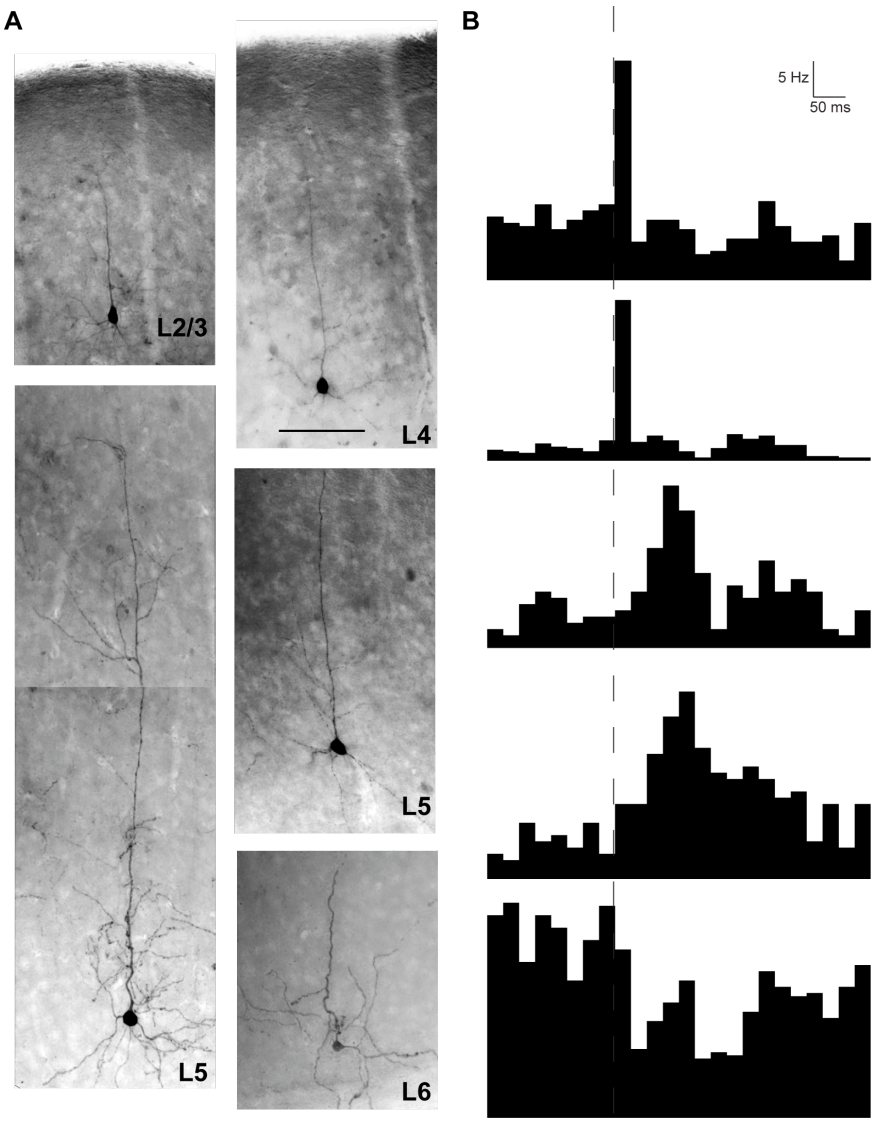

Figure S5. Related to Figure 5. Sound-activated units in L5 of V1. (A) Microphotographs of biocytin-filled, intracellularly recorded pyramidal cells in the various cortical laminae of V1. Left column, from top to bottom: a L2/3P and a L5P excited by sound; right column, from top to bottom: a L4P that was unresponsive to sound, and a L5P and a L6P that were hyperpolarized by sound. Calibration bar: 100 μm. (B) The first and second cell from the top show representative PSTHs of two V1 L5 neurons which fired in response to noise bursts within the first 50 ms from the acoustic stimulus onset. The third and fourth cells from the top show representative

PSTHs of two V1 L5 neurons which fired during the SH in V1 L2/3 Ps. Conversely, the fifth cell from top is inhibitited by sound.

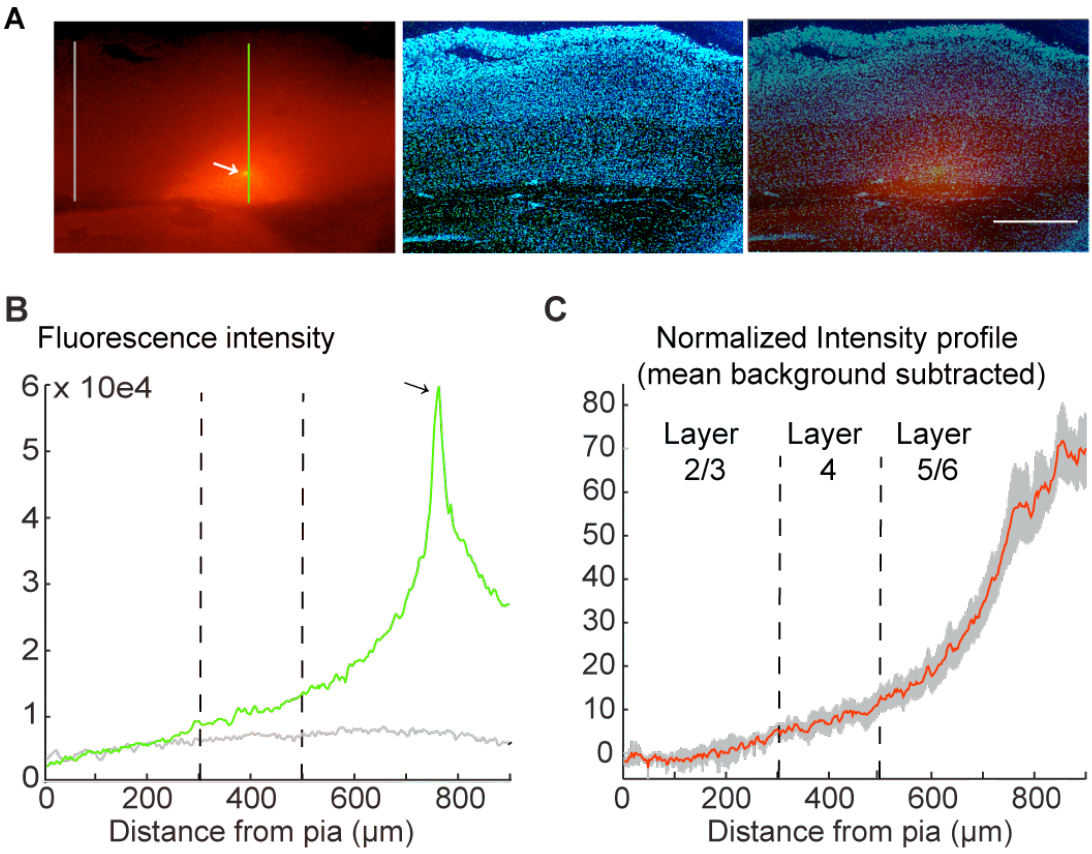

Figure S6. Intensity profiles along the cortical depth upon fluorescent muscimol injection in infragranular layers. Related to Figure 6. (A) Examples of microphotographs taken from a mouse injected with fluorescent muscimol in infragranular layers. The arrow indicates the putative injection site. Coronal sections were Nissl-counterstained to reveal layering (middle and overlay in right image). Bar: 500 µm. Fluorescence intensity was measured along two lines perpendicular to the pia, one centred on the injection spot (green line) and one outside it within the same section (background, gray line). Images were taken at 16 bits depth taking care to avoid pixel saturation. (B) Fluorescence intensity profiles along the two lines depicted in A. Note the lack of detectable diffusion of fluorescent muscimol in layer 2/3. (C) Grand average ± s.e.m of the normalized fluorescence intensity throughout all analysed slices (n = 6, the slice showing the brightest spot was chosen for every animal). The mean

value of the background fluorescence was subtracted in each slice. Note the concentration of fluorescent muscimol in infragranular layers, the white matter acting as barrier (Allen et al., 2008) and the absence of labelling in layers 2/3, indicating that muscimol did not diffuse to more superficial laminae. Layer borders were defined as based on the mean values taken from the Nissl counterstainings.

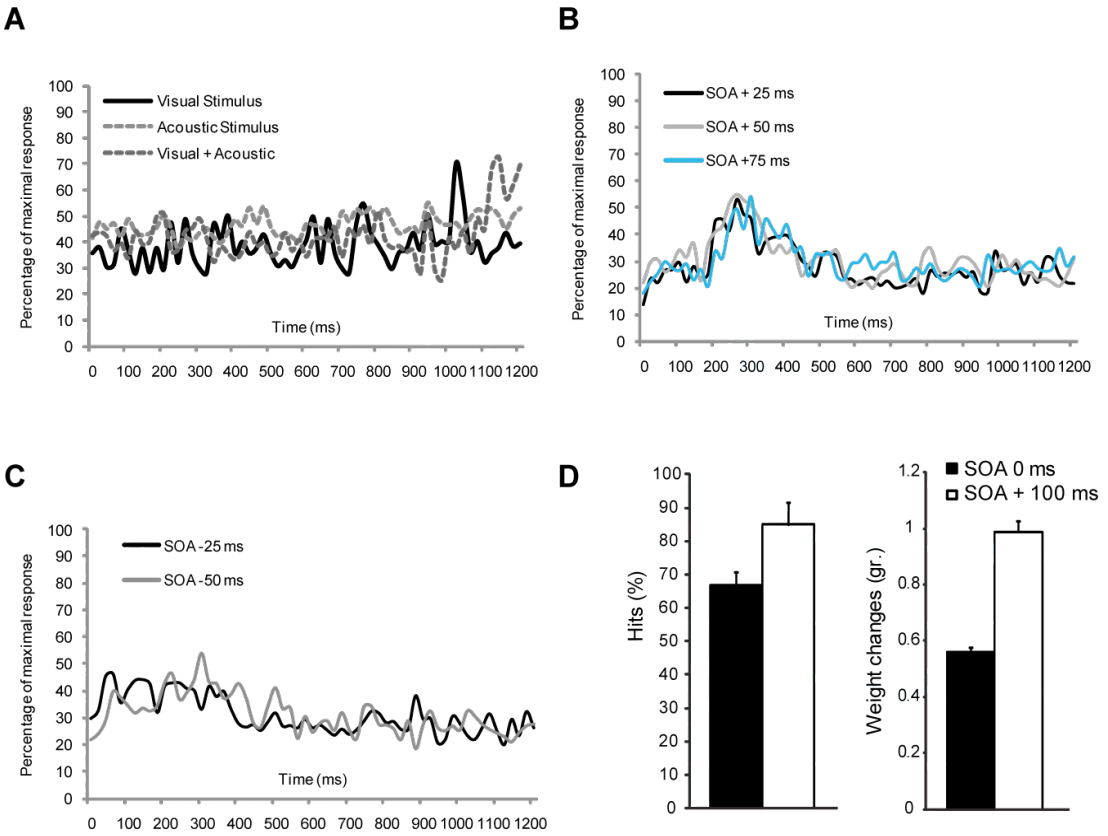

Figure S7. | Effects of SOA on acoustic inhibition of visually-driven CMRs and trial-by-trial analysis. Related to Figure 8. (A) The analysis of the motor activity in naive mice (N = 8) shows that they do not present any conditioned-like response (no peak motor activity) during the presentation of the visual, acoustic and visual + acoustic stimuli used in the conditioning experiments. Stimulus onsets: 50 ms. (B,C) Examples of the effects of sound on grand-averaged V-CMRs at positive (B) and negative (C) SOAs. (D) Trial-by-trial analysis of motor responses at SOAs 0 (where heteromodal suppression was observed) and +100 ms (where heteromodal suppression was not observed). The left plot shows the relative frequency of "hit" trials, defined as those trials in which the motor activity peak computed during the 200-400 ms time window was larger than baseline motor activity plus 3 standard deviations. The percentage of "hit" trials for SOA 0 ms is significantly lower compared to that measured for SOA +100 ms (65.0 ± 3.3 vs 85.0 ± 6.3 %, paired t-test, $p < 0.01$). Right

plot: the peak amplitude of the motor responses of the “hit” trials, measured as change of weight on the accelerometric platform, is significantly lower at SOA 0 ms compared to SOA +100 ms (0.96 ± 0.04 vs 0.51 ± 0.02 g, t-test, $p < 0.001$).

B. SUPPLEMENTAL EXPERIMENTAL PROCEDURES

1. Animal preparation and surgery

1.1 Lightly anaesthetized mice. All procedures were done accordingly to EU and Italian Ministry of Health regulations on animal welfare. C57BL/6J mice (4-6 weeks old) were anesthetized with urethane (0.8-1 g/Kg, i.p.) and implanted with a light-weight metal head holder and a recording chamber. Dexamethazone (0.01 mg/kg) was injected (i.m.) to prevent cortical and mucosal edema. Humidified oxygen was administered to the animal through a nose cannula, and body temperature was held at 37º C through a thermostatic blanket. Pinch reflexes, electrocardiogram (ECG) and breathing rate were continuously monitored during the experiment. For recordings in A1, the temporal muscle was infiltrated with lidocaine (1 %) and part of it carefully dissected around the area of interest. Eyelids were kept closed during experiments unless visual stimulation was performed. In the latter case, the contra-lateral eye position was controlled using a light metal ring: pupils projected at 50-55 deg lateral from the vertical meridian. Artificial tears were used to protect the cornea. 500 μm sized craniotomies and durotomies were opened in the position indicated by the ISI session. During recordings mice alternated between periods of quiet sitting and periods in which they groomed and whiskered spontaneously or upon room stimuli.

1.2 FP recordings in freely moving mice. 0.8-1 MΩ tungsten microelectrodes (FHC, Bowdoin, USA) were implanted 150 μm below the cortical surface of binocular V1 under isoflurane anaesthesia (1.5 %)(Frenkel et al., 2006). The electrode insertion point was covered with Kwik-Cast (World Precision Instruments Germany, Berlin, Germany) and the electrode was secured with acrylic cement. After 4-5 days of

recovery, chronically implanted mice were placed in a white plastic arena and exposed to acoustic stimuli.

1.3 In vivo pharmacology. *To inactivate A1*, about 300-400 nl of muscimol solution (10 mM in saline containing 5 % Fast Green) were injected in the position indicated by the ISI using a pressure injection system (Picospritzer III, Parker, Cleveland, OH, USA). A1 inactivation was verified using FP and multi-unit recordings in A1 in response to white noise bursts. To verify the extent of muscimol diffusion, some animals were quickly decapitated immediately after the injection, the brain was extracted and the cortical surface was observed under an epifluorescence, camera-equipped dissecting macroscope. Images were acquired and the radius of diffusion was measured (n = 3, ca 1 mm).

To inactivate GABAergic transmission locally in V1, extracellular solution containing 1.5 μM gabazine and/or 1 μM CGP52432 (as in (Murayama et al., 2009)) was applied on the exposed craniotomy. Recordings started after 30 minutes after drug application.

To inactivate layer 5 in V1 a local puff of 4 mM muscimol was given (estimated injection volume: ca 50 nl). To this aim, an extracellular pipette was located just above the putative layer 5/6 border. We always confirmed that spiking was locally abolished by means of subsequent multi-unit recordings. *In vivo* wc recordings were done within 30 minutes from the muscimol puff. To check diffusion of the drug, BODIPY TMR-X conjugated muscimol (Allen et al., 2008) was injected using the same protocol and, after in vivo wc recordings, animals were immediately transcardially perfused with 4% paraformaldehyde (PFA) in 0.1 M phoshate buffer (PB). Drug diffusion was checked on 100 μm-thick, vibratome-cut sections counterstained for Nissl.

Acute intracortical drug infusions in awake, behaving animals: C57BL/6J mice were anaesthetized with isofluorane (1-2 %) in O_2 mixture, delivered through a nose cone adapter. Body temperature was monitored and kept at 37 ºC with a homeothermic blanket control unit. Mice were positioned in a stereotaxic instrument with blunt ear bars (Kopf Instrument, CA, USA) with the head oriented at a 0º angle to the horizontal plane (flat skull). The skull was exposed, and two holes (one per hemisphere) were drilled 2.75 mm lateral to midline and 0 mm anterior to the Lambda. Stainless steel screws were used to secure the implant. Two 26-gauge stainless steel cannulae (UNIMED, CH, one per hemisphere) were lowered through the visual cortex to a depth of 0.3 mm ventral to the dura mater. The cannulae were affixed and kept in their position with dental cement. Mice were allowed for post-surgery recovery for at least 5-6 days before experiment. At the conclusion of each experiment, mice were deeply anesthetized and transcardially perfused with cold 0.9 % saline (pH 7.2), followed by cold 4 % paraformaldehyde (pH 7.2). Brains were removed and cryostat sections (30 μm thick) were collected and Nissl stained to verify the position of the injection site. Bilateral microinjections were performed as previously described(Carrasquillo and Gereau, 2007). Briefly, injections were performed using two 28-gauge injection cannulae extending 0.3 mm beyond the tip of the guide cannulae. After 5-6 days, the injection cannulae were attached to two separate 10 microliter syringes (Hamilton) by flexible plastic tubings. A total volume of 0.7 μl was infused over a period of 10 min by an infusion pump. The injection cannulae were kept in place for additional 5 min to allow for drug infusion. Injected drugs: picrotoxin, CGP 55845 hydrochloride, and Muscimol (Tocris Bioscience, Ellisville, MO, USA) were dissolved in saline at the concentrations of 100 μM, 3 μM and 1 mM, respectively. The concentration of PTX (100 μM) used here is known to alter only slightly cell responsiveness in rat V1 *in vivo*

(Harauzov et al., 2010). All drug solutions were freshly prepared on the day of the experiment. Vehicles were prepared according to the volumes of solvents used to dissolve the relative drugs. Behavioral experiments were done between 5 and 15 minutes from the end of the drug infusion.

1.4 Cortical Transections: transections between V1 and A1 were guided by the positions of the corresponding ISI spots and were done with a 30-gauge surgical blade run in rostrocaudal direction up to a depth of 1.5 mm from the pia. After 30-60 minutes from the transection, we checked that the transection did not affect both the visually-evoked and acoustically-evoked potentials in V1 and A1, respectively. At the end of the experiment, animals were transcardially perfused with 4% PFA in PB, and coronal sections were checked to verify the coronal level of the transection and that it reached the white matter.

2. Intrinsic signal imaging

V1, A1 and S1 (barrel cortex, D1 column) were located by performing intrinsic signal imaging (ISI) through the thinned bone. A vasculature ("green") image was acquired under 540 nm light before starting the imaging session. During ISI, the cortex was illuminated with monochromatic light of 630 nm wavelength. Images were acquired using a cooled 50 Hz CCD camera connected with a frame grabber (Imager 3001, Optical Imaging Inc, Germantown, NY, USA), defocused ca 500-600 μm below the pial surface. Data frame duration was 200 ms and a spatial binning of 3x3 was applied over the images, which were 4.35 x 4.35 mm. All image frames obtained during stimulus presentations were divided by the average image of the first 10 frames acquired just before stimulus presentation (Schuett et al., 2002). Data collection lasted 40 data frames after stimulus onset. Data collection included both stimulation and non-

stimulation (blank trials) randomly interlaced by the computer with a minimum inter-trial interval of 15 s. The relative decrease of reflectance, averaged over the stimulus presentation period, was then outlined. The spot area was taken as the image area where the visually-evoked decrease in reflectance was higher than 50% of the peak decrease. This region was then overlaid with the vasculature "green" image to open craniotomies.

3. Sensory stimulation

3.1 For intrinsic signal imaging. *Visual stimulation.* Eye bulbs were kept fixed with metal rings adjusted so that the eye pupils projected at ca 55-57 deg with respect to the vertical meridian. Corneas were protected with artificial tears. A 20 x 20 deg squared spot was projected in a position just lateral to the vertical meridian and 20 deg of elevation. The spot displayed squared drifting gratings (duration 8 s, spatial frequency 0.05 cycles/deg, speed 2 cycles/s, contrast 90%, mean grating luminance 19 cd/m^2). Stimulus orientation was randomly alternated during the 8 s of stimulation (every 45 degrees, every s), and stimuli were randomly interleaved with a full-field blank screen whose luminance was equal to the mean luminance of the grating (K0 blank). This same background surrounded the stimulus spot. Stimuli were displayed at 25 cm from the animal's eyes on a cathode ray tube monitor (22", Sony G520). *Auditory stimulation.* For each trial 4 noise bursts (72 dB SPL, 50 ms duration, 250 ms inter-burst interval) were presented to the controlateral ear. *Whisker stimulation.* All whiskers except D1 were trimmed; D1 whisker contralateral to the thinned skull was cannulated with a pipette glued to a piezoelectric device (Physik Instrumente GmbH, Karlsruhe, Germany) and deflected by about 8-10 deg at 10 Hz for 2 seconds in a rostro-caudal direction.

3.2 For electrophysiology experiments. *Acoustic stimuli* were delivered every 5-7 s through a speaker located 8 cm in front of the contra-lateral ear. Stimuli consisted of noise bursts (frequency range: 3-20 kHz, 50 ms, 72 dB SPL). Room noise level was 35 dB SPL. Sound intensities and background levels were measured using a phonometer (Chauvin Arnoux, model CA834; correction curve: 'A' frequency weighting). For the intensity-response experiments, the different sound intensities were presented in random order. *Visual stimuli* were delivered every 5 s with the screen positioned at 25 cm from the mouse's eyes. 3 deg wide moving light bars (luminance 20 cd/m^2, background luminance 2 cd/m^2, angular speed 45-55 deg/s) of different orientations (every 45 deg) were presented to the contra-lateral eye. For multimodal stimulation experiments, only responses to the cell preferred orientation and direction were considered. Alternatively, a 20x20 deg-wide squared spot was flashed in a position centered on the retinotopic spot identified by ISI. Luminance settings were the same as for the moving bar stimulation. *Whisker stimulation:* caudal whiskers (C to E rows) were stimulated by computer-controlled movements of piezoelectric wafers and consisted of single high-velocity deflections in the dorsal direction (10 degrees, delivered every 5-7 s). Steps elicited by the piezoelectric device had a 10-90 % rise time of 1 ms.

4. Optogenetic and electrical stimulation

4.1 Optogenetic stimulation: Thy1::ChR2-EYFP line 18 transgenic mice (4-6 weeks old) were obtained from The Jackson Laboratory. Photo-stimulation of layer 5 cortical neurons was obtained by coupling a multimodal optical fiber (core diameter 200 µm, NA 0.22, OZ Optics Limited, Ottawa, Canada) to a 100 mW blue (473 nm) TTL controlled laser (SDL-473-100T, Shanghai Dream Lasers Technology Co., Shanghai,

China). Light power delivered at the end of the fiber (20 mW/mm^2) was measured using a power meter (PM120 with S121C sensor, Thorlabs Inc., Newton, NJ, USA) to remain in a safe range for *in vivo* experiments (Cardin et al., 2010). The optical fiber was placed just above the exposed brain surface and 1 ms light pulses were triggered by a TTL control signal every 5 s. The animal eyes were closed during photo-stimulation.

4.2 Electrical microstimulation:

Cortical microstimulation was done with Tungsten bipolar concentric electrodes (FHC, Bowdonian, USA, outer-inner diameters: 250-30 μm) within a 600-800 μm craniotomy in area V1. Stimulation intensity was set to 50% with respect to the levels giving rise to saturating responses, as assessed by previous FP measurments (average stimulus intensity: 300 μA). For wc recordings, 20 sweeps were averaged before and after perfusion with PTX/Cs containing intracellular solution, stimulation frequency and pulse duration were set to 0.2 Hz and 1 ms, respectively.

5. Electrophysiological recordings

5.1 Extracellular recordings

Extracellular recordings were done with 2-3 MΩ glass pipettes filled with normal Ringer's solution (in mM: 135 NaCl, 5.4 KCl, 1.8 $CaCl_2$, 1 $MgCl_2$) or with 1 MΩ tungsten electrodes in awake, freely moving mice. The extracellular pipette was positioned within the craniotomy (500 μm wide) within a distance of 200-300 μm from the patch electrode. Craniotomies were perfused with Ringer solution warmed at 37° C. For FP recordings, the signal was amplified (5000x) and band-filtered (0.1-300 Hz).

Stimuli were presented 30-50 times every 6 seconds and responses were trigger-averaged. For multi-unit recordings, the signal was band-filtered (0.5-5 kHz) and amplified (gain 5000x). For single-unit recordings, single APs were isolated in juxtasomal configuration (de Kock et al., 2007). After observing an increase of electrode resistance, the electrode was advanced stepwise (1-2 μm) until positive AP waveforms were recorded with amplitudes of 1–3 mV. Data were sampled at 10 kHz except for freely moving animals (5 kHz).

5.2 Tetrode recordings. Mice were implanted in the visual cortex with an array of four silicon-iridium tetrode probes for acute recordings (A 4 x 1-Tet-3mm 150-312, Neuronexus Technologies, Ann Arbor, MI), and electrophysiological signals were acquired and digitized at 32 kHz employing a Digital Lynx 4S recording system (Neuralynx, Bozeman, MT).

5.3 Whole-Cell Recordings. 5-9 MΩ borosilicate patch pipettes filled with intracellular solution (in mM: 135 K gluconate, 10 HEPES, 10 Na phosphocreatine, 4 KCl, 4 ATP-Mg, 0.3 GTP, pH 7.2, 2 mg/ml biocytin, 291 mOsm) were lowered perpendicularly to the pia by applying ca 300 mmHg of positive pressure until the layer of interest was reached (Margrie et al., 2002). For intracellular perfusion experiments, K^+ ions were substituted by Cs^+ ions and 1 mM picrotoxin (PTX) was added(Nelson et al., 1994; Yazaki-Sugiyama et al., 2009). To minimize picrotoxin spillover, pipette tips were filled with PTX-free intracellular solution and pipettes were backfilled with the PTX containing solution. In addition, the positive pressure applied to the pipette to advance through the cortex was diminished to 150-200 mmHg or not applied at all. Cells recorded under PTX/Cs depolarized to resting values between -45 and -20 mV within 5-10 minutes. Cells were searched in voltage clamp mode with the positive pressure lowered to 30 mmHg while moving the micromanipulator in 2 μm steps along the

pipette axis. On approaching a cell, pressure was relieved and light suction was applied to allow gigaseal formation. After capacitance compensation, a ramp of negative pressure usually led to wc configuration. Recordings were performed with an EPC10 double plus amplifier (HEKA, Germany) operated in current clamp (voltage follower mode) and the V_m signal was digitized at 20kHz and acquired using the program Patchmaster (HEKA, Germany). Seal resistance was higher than 2 GΩ, and spike height and overall V_m were stable throughout recordings. No holding current was used unless estimates of synaptic conductances were performed. Series resistance was repeatedly monitored, compensated for and ranged 10-100 MΩ. For conductance measurements, series resistance compensation was made offline. Recording durations in lightly anaesthetized mice ranged from 20 minutes to 2 hours. 1-2 whole cell recordings were performed per animal.

6. Data Analysis

6.1 Spectral analysis. We computed the magnitude FFT for the V_m and FP signals with Igor Pro (WaveMetrics, USA) over 5 s segments of spontaneous activity per cell. APs were removed by linear interpolation based on AP duration. The FFT of the FPs was normalized by its integral. To quantify the depth of anaesthesia, we calculated the ratio between the area in the 1-5 Hz range (low frequency, LF) and the area in the 10-40Hz range (high frequency, HF) of the V_m FFT spectra (Crochet and Petersen, 2006; Li et al., 2009). *Spectograms and coherence analyses* of sound-driven responses were performed on down-sampled z-scored traces (0-500Hz) using a multitaper spectral estimation method over a moving window with the "newtimef" function in the Matlab toolbox EEGLab (http://sccn.ucsd.edu/eeglab/)(Delorme and Makeig, 2004). Briefly,

time-frequency power spectra were computed by means of Fast Fourier Transform computed over a moving Hanning window. Inter-trial coherence was computed as the phase-locking factor for each time-frequency window. Statistical deviations from baseline were computed with a bootstrap method (Delorme and Makeig, 2004).

6.2 Spike sorting on tetrode recordings

Signals were processed via custom off-line algorithms in MatLab ® (The MathWorks Inc., Natick, MA). Signals were first average referenced (no reference electrode was employed) and then filtered in the 500 Hz-10 kHz range for spike detection. Spikes were extracted by manually setting a threshold for each channel at approximately 3-4 times the standard deviation of background noise (Lewicki, 1998; Tolias et al., 2007; Vyazovskiy et al., 2009). For each spiking event, 64 samples were extracted, from -0.65 ms to +1.29 ms around spike peak. Spike sorting was performed following (Tolias et al., 2007). For each recording site, principal components analysis (PCA) was performed on recorded spike waveform data, and the first 3 principal components (PCs) were employed in subsequent analyses, after verifying that they were able to account for at least 70% of all variance. Unsupervised clustering was then performed on the computed 12 PCs (3 for each of the recording sites), by employing split and merge expectation maximization (SMEM, (Ueda et al., 2000)). In SMEM a mixture of Gaussian distributions is initially fitted to the data set by expectation maximization. Then individual Gaussian distributions are iteratively split and merged until convergence of the likelihood function to a maximal value is achieved. The SMEM algorithm has been successfully employed for spike sorting (Tolias et al., 2007; Vyazovskiy et al., 2009), since it is less prone than other algorithms to converge to local maxima. The results of the clustering algorithm were always carefully checked,

both visually and by means of quantitative indexes. Visual inspection was always necessary to discard cluster corresponding to artifacts and – eventually – merge or discard poorly isolated units. Quality of isolation was verified for each cluster by computing a false positive/false negative index (Tolias et al., 2007). A set of simulated PC data points was generated from the fitted mixture of Gaussians, thus knowing a priori to which cluster each point belonged. Then, each point was a posteriori assigned to a cluster and the ratio of false positives and false negatives was computed. Clusters for which this ratio exceeded 0.05 were excluded as poorly isolated. Finally, if necessary, the SMEM procedure was repeated several times, and the result having the highest Bayesian information criterion (BIC) index (computed on a subset of data kept for testing purposes) was selected(Tolias et al., 2007).

***6.3 Analysis of sensory responses*:**

-In vivo whole-cell. Data were analyzed using custom-made software written in IgorPro or MatLab. For the analysis of sub-threshold responses, APs were truncated using linear interpolation and sweeps were averaged. *PSP amplitude* was computed with respect to the mean V_m during the inter-stimulus period after averaging sweeps. Unless otherwise stated, PSP amplitudes were taken in the 0 – 300 ms poststimulus time window as the largest hyperpolarization compared to the baseline level in case of hyperpolarizing responses, or as the largest depolarization when a depolarizing postsynaptic potential was observed. Onset latency of postsynaptic responses was measured at the time point where the amplitude of the signal was larger than the averaged resting V_m plus 2 standard deviations of the baseline values. To compute the amplitude of visually evoked *AP responses*, mean spontaneous AP rates were subtracted. To compute PSTHs of AP counts, 50 ms binning was applied for patch recordings. The *total number of APs per stimulus passage* was calculated inside the

cell RF, as defined by the region of space whose stimulation increased AP firing over mean spontaneous firing rate + 2 standard deviations (Pizzorusso et al., 2002). *Reliability* of supra-threshold visual responses was quantified by computing the coefficient of variation of AP counts in response to the stimulus on a single trial basis (de Kock et al., 2007).

-*Tetrode extracellular recordings.* For every sorted unit, spike trains were constructed for each trial in a time frame ranging from -500 ms to +1000 ms around stimuli. Spike trains were defined as time series having 0 value everywhere but in those samples corresponding to the occurrence of a spike peak, where value was set to 1. Trials affected by noise or artifacts were excluded from the analysis. For each neuron instantaneous firing rates (in Hertz) were computed by performing a convolution between spike trains and a Gaussian window with a standard deviation equal to 50 ms (Rieke et al. 1999). Such firing rates were then averaged across all trials.

6.4 Assessment of changes in input resistance and excitatory and inhibitory conductances

The time course of changes in input resistance was measured by fitting the relation between the membrane potential, $V_m(t)$, and the injected current, $I_{inj}(t)$, at each instant to equation

$$V_m(t) = V_0(t) + I_{inj}\, R(t)$$

where R(t) is the input resistance at time t and $V_0(t)$ is a linear estimate of the membrane potential recorded without injected current(Anderson et al., 2000). I_{inj} is the injected current: 3 to 5 currents were injected (from -200 pA to 100 pA, mostly hyperpolarizing).

Synaptic conductances were estimated through a standard linear method based on the fundamental membrane equation(Anderson et al., 2000; Monier et al., 2003; Priebe and Ferster, 2005).

$$g_e(t)\,(V_m(t) - E_e) + g_i(t)\,(V_m(t) - E_i) = -C\,dV_m(t)/dt - g_{rest}\,(V_m(t) - E_{rest}) + I_{inj}$$

g_e and g_i are the excitatory and inhibitory synaptic conductance changes with respect to the resting, unstimulated state, respectively. E_e (0 mV) and E_i (-90 mV) are the reversal potentials for excitation and inhibition, respectively. The latter is intermediate between the equilibrium potentials of $GABA_A$ and $GABA_B$ channels according to the ionic composition of our intracellular solution. E_{rest} was the median V_m value during baseline (no stimulus) recording without current injection. V_m and dV_m/dt are the recorded membrane potential and its derivative at any time point, respectively. C and g_{rest} are the membrane capacitance and resting conductance, respectively; they were calculated by least square fitting of the double exponential

$$V_m(t)/I_{pulse} = [1 - \exp(-t / t_s)]/g_s + [1 - \exp(-t / t_{rest})]/g_{rest}$$

to the responses to 50 current pulses (I_{pulse} from -200 pA to 100 pA, 100 ms), each given before stimulus presentation. t_{rest} and t_s are the time constants of the membrane and of the patch electrode, respectively. g_s is the inverse of the series resistance. To compensate for the series-resistance, $V_m(t)$ was further corrected offline by:

$$V_m(t) = V_m(t) - I_{inj} / g_s$$

The accuracy of our estimates was assessed by recontructing the V_m waveform from the estimated g_e and g_i values (see Supplementary Figure 2). Our estimates accounted for 94 % of the variance across all neurons.

7. Behaviour

C57Bl/6J male mice (10 weeks old) were subjected to a conditioning phase consisting of a series of temporal pairings of a visual signal with an electric shock (20 pairings, intertrial time 1 minute, delivered current: 100 ms at 0.1 mA). The electric shock occurred after 250 ms from a 50 ms flash (from a 40 LUX house light to a 50 LUX caused by a LED). After 24 hours from the conditioning phase, the conditioned motor response (CMR) was measured by presenting visual stimuli again (visual probes). Among visual probe trials, we introduced in random order trials where the flash and the acoustic stimulus (50 ms white noise) were presented together at different stimulus onset asynchronicities (SOAs) to document the effects of acoustic stimuli on the visually-driven CMR (audio-visual probes). Sounds were introduced in the testing chamber by two synchronised speakers. Chambers were acoustically isolated and their background noise was 30 dB SPL. The sound intensity used for behavioural experiments was 65 dB SPL. Each mouse was tested in one fully equipped testing chamber. The mouse was housed in a small metal frame positioned on a platform which allows the detection of motor responses. The testing chambers, the stimulation apparatus and computer software were developed by TSE (Bad Homburg, Germany). A weight sensor integrated in the measuring platform allowed accurate measurements of the animal's reactions. The movement data of an animal is calculated by indirectly measuring its acceleration on the platform. This was done by determining the changes

in force exerted on the platform by the animal's movements (expressed in grams). Data were sampled every 2 ms and time-binned every 10 ms. Single trial responses within each experimental condition, have been averaged for each animal. The time course of the locomotor activity have been then normalized to their absolute peaks to take into account interindividual differences. Statistical comparisons have then been done between the normalized peaks measured within the time window during which the electric shock was expected (200-400 ms) (Tucci et al., 2006). For the analysis of single trial responses, a trial was considered "hit" or "missed" if the motor activity peak computed during the 200-400 ms time window was larger than baseline motor activity plus 3 standard deviations. For stimulus intensity-response curves, experiments were done were heteromodal suppression was maximal (SOA = 0 ms) and the different sound intensity were paired randomly with the light stimulus. In the case of acute intra-cortical infusions with cannulae implants, baseline motor activity was similar for mice injected with vehicle or PTX-CGP55845 (means ± s.e.m.: 0.27 ± 0.03 vs 0.22 ± 0.03 grams, respectively; t-test, $p = 0.23$). No sign of epileptic activity was ever seen in any of the recorded animals (see also(Harauzov et al., 2010)).

8. Histochemical Staining and Neuronal Identification:

At the end of the recording sessions, animals were deeply anesthetized with urethane (i.p.) and transcardially perfused with 60 ml cold (4° C) phosphate buffer 0.1 M followed by 120 ml of 4% paraformaldehyde in 0.1 M phosphate buffer. Brains were postfixed in 2% paraformaldehyde in 0.1 M phosphate buffer overnight. 100 μm thick coronal sections were cut using a vibratome, stained for biocytin to reveal recorded neurons and counterstained for cytochrome oxidase to reveal layer 4 (Tsiola

et al., 2003). Sections were then mounted with Mowiol and recorded pyramidal neurons were classified according to the laminar position of their somata.

C. OTHER SUPPLEMENTAL TEXT

Author Contributions. G.I. did all electrophysiological experiments and analyzed data, D.G. did some extracellular physiology experiments and the photo-stimulations, U.O. analyzed extracellular recordings of spiking activity and did part of the intracellular recordings, G.L. and V.T. did and analyzed the behavioural experiments, C.N. and R.T. did the acute pharmachology in the behavioural experiments, P.M. directed the study, designed the experiments with the contribution of all authors, analyzed data and wrote the manuscript with F.B and G.I

D. SUPPLEMENTAL REFERENCES

Allen, T.A., Narayanan, N.S., Kholodar-Smith, D.B., Zhao, Y., Laubach, M., and Brown, T.H. (2008). Imaging the spread of reversible brain inactivations using fluorescent muscimol. J Neurosci Methods *171*, 30-38.

Anderson, J.S., Carandini, M., and Ferster, D. (2000). Orientation tuning of input conductance, excitation, and inhibition in cat primary visual cortex. J Neurophysiol *84*, 909-926.

Cardin, J.A., Carlen, M., Meletis, K., Knoblich, U., Zhang, F., Deisseroth, K., Tsai, L.H., and Moore, C.I. (2010). Targeted optogenetic stimulation and recording of neurons in vivo using cell-type-specific expression of Channelrhodopsin-2. Nat Protoc *5*, 247-254.

Carrasquillo, Y., and Gereau, R.W.t. (2007). Activation of the extracellular signal-regulated kinase in the amygdala modulates pain perception. J Neurosci *27*, 1543-1551.

Crochet, S., and Petersen, C.C. (2006). Correlating whisker behavior with membrane potential in barrel cortex of awake mice. Nat Neurosci *9*, 608-610.

de Kock, C.P., Bruno, R.M., Spors, H., and Sakmann, B. (2007). Layer- and cell-type-specific suprathreshold stimulus representation in rat primary somatosensory cortex. J Physiol *581*, 139-154.

Delorme, A., and Makeig, S. (2004). EEGLAB: an open source toolbox for analysis of single-trial EEG dynamics including independent component analysis. J Neurosci Methods *134*, 9-21.

Frenkel, M.Y., Sawtell, N.B., Diogo, A.C., Yoon, B., Neve, R.L., and Bear, M.F. (2006). Instructive effect of visual experience in mouse visual cortex. Neuron *51*, 339-349.

Harauzov, A., Spolidoro, M., DiCristo, G., De Pasquale, R., Cancedda, L., Pizzorusso, T., Viegi, A., Berardi, N., and Maffei, L. (2010). Reducing intracortical inhibition in the adult visual cortex promotes ocular dominance plasticity. J Neurosci *30*, 361-371.

Lewicki, M.S. (1998). A review of methods for spike sorting: the detection and classification of neural action potentials. Network *9*, R53-78.

Li, C.Y., Poo, M.M., and Dan, Y. (2009). Burst spiking of a single cortical neuron modifies global brain state. Science *324*, 643-646.

Margrie, T.W., Brecht, M., and Sakmann, B. (2002). In vivo, low-resistance, whole-cell recordings from neurons in the anaesthetized and awake mammalian brain. Pflugers Arch *444*, 491-498.

Monier, C., Chavane, F., Baudot, P., Graham, L.J., and Fregnac, Y. (2003). Orientation and direction selectivity of synaptic inputs in visual cortical neurons: a diversity of combinations produces spike tuning. Neuron *37*, 663-680.

Murayama, M., Perez-Garci, E., Nevian, T., Bock, T., Senn, W., and Larkum, M.E. (2009). Dendritic encoding of sensory stimuli controlled by deep cortical interneurons. Nature *457*, 1137-1141.

Nelson, S., Toth, L., Sheth, B., and Sur, M. (1994). Orientation selectivity of cortical neurons during intracellular blockade of inhibition. Science *265*, 774-777.

Pizzorusso, T., Medini, P., Berardi, N., Chierzi, S., Fawcett, J.W., and Maffei, L. (2002). Reactivation of ocular dominance plasticity in the adult visual cortex. Science *298*, 1248-1251.

Priebe, N.J., and Ferster, D. (2005). Direction selectivity of excitation and inhibition in simple cells of the cat primary visual cortex. Neuron *45*, 133-145.

Schuett, S., Bonhoeffer, T., and Hubener, M. (2002). Mapping retinotopic structure in mouse visual cortex with optical imaging. J Neurosci *22*, 6549-6559.

Tolias, A.S., Ecker, A.S., Siapas, A.G., Hoenselaar, A., Keliris, G.A., and Logothetis, N.K. (2007). Recording chronically from the same neurons in awake, behaving primates. J Neurophysiol *98*, 3780-3790.

Tsiola, A., Hamzei-Sichani, F., Peterlin, Z., and Yuste, R. (2003). Quantitative morphologic classification of layer 5 neurons from mouse primary visual cortex. J Comp Neurol *461*, 415-428.

Tucci, V., Hardy, A., and Nolan, P.M. (2006). A comparison of physiological and behavioural parameters in C57BL/6J mice undergoing food or water restriction regimes. Behav Brain Res *173*, 22-29.

Ueda, N., Nakano, R., Ghahramani, Z., and Hinton, G.E. (2000). SMEM algorithm for mixture models. Neural Comput *12*, 2109-2128.

Vyazovskiy, V.V., Olcese, U., Lazimy, Y.M., Faraguna, U., Esser, S.K., Williams, J.C., Cirelli, C., and Tononi, G. (2009). Cortical firing and sleep homeostasis. Neuron *63*, 865-878.

Yazaki-Sugiyama, Y., Kang, S., Cateau, H., Fukai, T., and Hensch, T.K. (2009). Bidirectional plasticity in fast-spiking GABA circuits by visual experience. Nature *462*, 218-221.